Ecological Indicators 158 (2024) 111488

Contents lists available at ScienceDirect

Ecological Indicators

journal homepage: www.elsevier.com/locate/ecolind

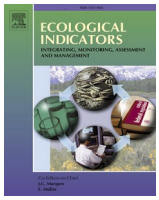

Original Articles

Agricultural land management extends the duration of the impacts of extreme climate events on vegetation in double–cropping systems in the Yangtze–Huai plain China

Tiexi Chen [a,b,c,*], Jie Dai [a], Xin Chen [a], Chuanzhuang Liang [a], Tingting Shi [d], Yanran Lyu [a], Fang Zhao [e], Xiuchen Wu [f], Miaoni Gao [a], Jinlong Huang [a], Shengjie Zhou [a], Han Dolman [g]

[a] School of Geographical Sciences, Nanjing University of Information Science and Technology, Nanjing 210044, China
[b] Qinghai Provincial Key Laboratory of Plateau Climate Change and Corresponding Ecological and Environmental Effects, Qinghai University of Science and Technology, Xining 810016, Qinghai, China
[c] Geographical Science, Qinghai Normal University, Xining, 810016, China
[d] School of Applied Meteorology, Nanjing University of Information Science and Technology, Nanjing 210044, China
[e] School of Geographic Sciences, East China Normal University, Shanghai, 200241, China
[f] State Key Laboratory of Earth Processes and Resource Ecology, Beijing Normal University, Beijing, 100875, China
[g] NIOZ Royal Netherlands Institute for Sea Research, Texel, The Netherlands

ARTICLE INFO

Keywords:
Climate extremes
Double–cropping
Land management
Vegetation

ABSTRACT

Extreme climate events can have severe impacts on both vegetation and the carbon cycle. However, whether land management exacerbates or mitigates the effects of extreme climate events on vegetation remains unknown. We investigated the case of an extreme precipitation event that occurred in a region dominated by double–cropping (DC) systems located in the Yangtze–Huai plain in China. Waterlogging disasters were triggered by an extreme precipitation event in October 2016, which severely affected the sowing and seedling emergence of winter crops (mainly winter wheat). The lack of sowing and low seedling emergence rate subsequently led to months of low growth, as evidenced by negative enhanced vegetation index (EVI) anomalies, especially from March to May 2017. Local agricultural meteorological monthly reports, government announcements, and winter wheat data based on statistics and remote sensing confirmed the reduced yields. The influence on vegetation ended in June 2017, when summer crops were planted. Our results demonstrate that, in such a DC system, when extreme events occur during the key sowing period, the impacts will continue through the entire crop growth period, until the next sowing. More generally, agricultural land management could extend the duration and magnitude of the impacts of extreme climate events on vegetation.

1. Introduction

Climate extremes, referring to the statistically unusual climate condition which could affect an ecosystem function outside the considered normal bounds (Reichstein et al., 2013; Smith, 2011), have reduced national cereal production by at least 9–10 % worldwide (Lesk et al., 2016). Such extremes are increasing in frequency, intensity, and duration according to historical records and projections employing state–of–the–art models (AghaKouchak et al., 2014; Easterling et al., 2000; Fischer et al., 2013; Katz, 2010; Sillmann et al., 2013; Zhai et al., 1999). Specific attention has been given to the impacts of climate extremes on terrestrial ecosystems (Jabal et al., 2022; Piao et al., 2019; Reichstein et al., 2013; Ummenhofer and Meehl, 2017; Wu et al., 2018; Yin et al., 2020), as terrestrial ecosystems serve as the biggest carbon sinks for regulating climate change (Ciais et al., 2014; Friedlingstein et al., 2019; Pan et al., 2011), and further provide most of the basic food services (Tilman et al., 2011; Vermeulen et al., 2012).

The mechanisms by which climate extremes impact ecosystems are diverse, since specific impacts are often the result of a combination of different climate extremes and a certain ecosystem type (Reichstein et al., 2013). Typical climate extremes, including drought, heavy rain, heat waves, cold waves, and snowstorms are frequently recurrent, and typically severely damage vegetation. Some ecological disasters can be triggered by such extremes, including tree mortality, wildfires, and

* Corresponding author.
E-mail address: txchen@nuist.edu.cn (T. Chen).

https://doi.org/10.1016/j.ecolind.2023.111488
Received 24 September 2023; Received in revised form 28 November 2023; Accepted 20 December 2023
Available online 6 January 2024

insect infestations (Allen et al., 2010; Anderegg et al., 2012; Bowman et al., 2017).

Land management refers to the activities applied on land resources within a certain type (different from land cover/use change) (Chen et al., 2022a, 2022b; Erb et al., 2016; Luyssaert et al., 2014; Zhou et al., 2022). Take cropland as an example, land management includes multiple cropping, fertilizer usages, irrigation, agricultural machination and so on. Theoretically, land management could mitigate or exacerbate the impact of climate extremes on vegetation. A notable example is the impact of extreme drought events on vegetation in Russia in 2010, which was regulated by forest management and crop rotation (Loboda et al., 2017).

The most intense land management usually occurs in croplands, especially in the multiple cropping systems, which directly leads to the huge difference between the phenology of the crops and the natural vegetation (Chen,et al., 2016; Gaba et al., 2015). Double cropping (DC) systems involve planting on a given cropland twice during a calendar year, and are commonly used worldwide to enhance crop production (Siebert et al., 2010; Yan et al., 2014). As a result of global warming, the growing season in mid–latitude regions is lengthening, and the cultivated areas that are suitable for DC systems have expanded significantly (Liu et al., 2013; Seifert and Lobell, 2015). There are two transition (harvest–sowing) periods in the DC system. In order to ensure sufficient growth periods and guarantee yields, DC systems generally necessitate strict control over the time of harvest and sowing.

DC planting can be classified as a form of land management, as there is no change in land cover type. Usually, for single–cropping systems, if there is a failure in sowing due to disasters, reseeding is a reasonable and common recovery strategy (Bussmann et al., 2016; Marteau et al., 2011). However, for a two–season rotation system consisting of overwinter crops, the two sowing periods are fixed, each within a relatively narrow period of about one month. Once the optimal sowing period is missed due to extreme weather events, farmers are more inclined to simply not sow. Therefore, in theory, extreme events that occur during the transition periods may interfere with sowing and generate long–lasting negative effects. However, there have been few studies investigating the effects of extreme climate events on vegetation growth of DC systems. Therefore, a robust case is needed to establish a comprehensive logical chain, proving the impact of land management on DC agricultural systems during extreme events. One crucial metric in this regard is quantifying the duration of this impact. Clarifying this process helps enhance the ability of vegetation models to deal with land cover type of cropland, especially considering the influence of land management.

In this paper, we investigate a potential benchmark case in the Yangtze–Huai plain in China, whereby we aim to provide insights into the mechanism of the impacts of an extreme precipitation event during the sowing period on the vegetation of DC croplands. The plain under study is located in the eastern part of China, and is dominated by the East Asia Summer Monsoon. DC systems are widespread in this area (Chen et al., 2016; Yan et al., 2014). The winter crops planted in late autumn and harvested in summer are mainly winter wheat, with lesser amounts of rapeseed. The summer crops planted in the plain differ from north (dryland crops such as maize, soybean, and cotton) to south (paddy rice). The objective of this study is to understand further the integrated impact on ecosystem from the combination of climate extremes and specific land management.

2. Methods

2.1. Study area

The study region is located in the Yangtze–Huai plain (Fig. 1a) of Eastern China, covering a rectangular area between 30°N–36°N and 112°E–123°E. The topography is illustrated in Fig. 1a, using Global 30 Arc–Second Elevation (GTOPO30) (USGS, 1996). Plains dominate the area, although there are a few mountainous areas, including Mount Tai in Shandong Province, and the Dabie and Yellow Mountains in the south of Anhui Province.

This region is dominated by the East Asian monsoon with precipitation concentrated in the summer monsoon season. During the last decade (take 2009–2018 as a reference), the annual precipitation exceeded 1000 mm and temperature in the coldest month is still above 1 °C. DC systems are the main cropping types in this region (Yan et al., 2014), and can further be roughly divided into paddy field DC systems in the south and dry cropland DC systems in the north (Fig. 1b). ‘Paddy rice–winter wheat’ is the dominant combination in the paddy field DC systems, followed by ‘paddy rice–rapeseed’ and a small proportion of ‘paddy rice–paddy rice’. In the dry croplands, ‘summer crops–winter wheat’ is the main type of DC system. Summer crops mainly include corn, soybean, and cotton (Ho et al., 2012). The spatial distribution of these two types of DC systems is roughly the same as paddy field and dry field in land use classification (Fig. 1b, Table1). The letter S in Fig. 1 indicates the Shouxian National Climate Observatory, which is a typical ‘winter wheat–paddy rice’ DC cropland.

2.2. Datasets

We use the enhanced vegetation index (EVI) to describe vegetation

Table 1
Land cover types corresponding to Fig. 1b, and the land–cover percentages of each component of the area bounded by the red curve.

Class	Class Name	%
1	Paddy field	37.67
2	Dry field	30.52
3	Woodland and grassland	5.11
4	Water body, including natural land waters and land for water–conservancy facilities	12.18
5	Built–up land	14.49
6	Unused land	0.03

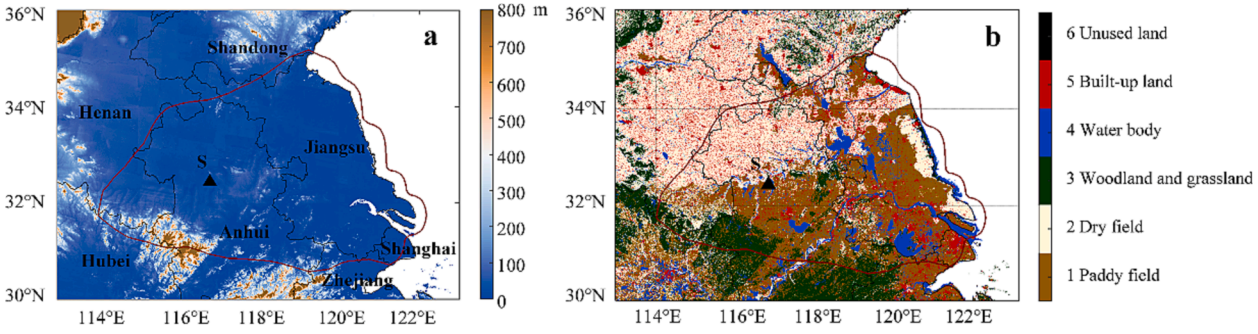

Fig. 1. Topography (a) and land cover (b) of the study area. Type 1–6 are Paddy field, Dry field, Woodland and grassland, Water body, Built–up land and Unused land respectively. The extent of the area covered by extreme precipitation events is illustrated by the red line (see the details in section 2.3).

conditions, which is a widely used method (Huete et al., 2002). Compared with NDVI (Normalized Difference Vegetation Index), EVI is proposed to overcome the saturation effect of NDVI and reduce both atmospheric and soil background noises (Huete et al., 2002). In addition, EVI can also reflect the change of crop yield to a certain extent, which has been well proved in previous studies (Bolton & Friedl, 2013; Karthikeyan et al., 2020; Skakun et al., 2017).

The monthly 1–km resolution MODIS EVI (MOD13A3) data were obtained from the LAADS DAAC (Level–1 and Atmosphere Archive & Distribution System Distributed Active Archive Center; https://ladsweb.modaps.eosdis.nasa.gov). The study region was divided into two tiles, h27v05 and h28v05, in a sinusoidal projection.

In order to reduce the uncertainty of EVI in representing of vegetation conditions and crop yield, solar induced chlorophyll fluorescence (SIF) data was further used. A large number of studies have demonstrated a strong correlation between SIF and crop yield (Guan et al., 2016; Cao et al., 2021; Peng et al., 2020). Here, three SIF data sets were used to increase the robustness of SIF changes, including two SIF data sets (GOSIF and CSIF), which are widely used to estimate crop yield, and one SIF data set developed based on TROPOMI SIF (RTSIF) (Chen et al., 2022c; Li & Xiao, 2019; Zhang et al., 2018). These data sets all have a spatial resolution of 0.05 degree.

Daily and monthly 0.5–degree gridded precipitation and temperature records were obtained from the China Meteorological Administration (CMA) (https://data.cma.cn/). This dataset was generated from observation data from more than 2,000 weather stations across the country. Therefore, it is one of the most accurate public datasets available for this study region (Xu et al., 2009).

Besides precipitation and temperature records, soil moisture data from various resources were selected using the methods of remote sensing, land model and reanalysis. Soil moisture from European Space Agency (ESA) Climate Change Initiative (CCI) is a long–term remote sensing–based soil moisture data which could represent the surface moisture condition (Liu et al., 2012) (https://www.esa-soilmoisture-cci.org/). Meanwhile, it has been well demonstrated that surface soil moisture can also reflect the water constraints on terrestrial ecosystems (Chen et al., 2014). Soil moisture of the top 28 cm from ERA5 reanalysis (Hersbach et al., 2018) (https://cds.climate.copernicus.eu/) and root zone soil moisture from GLEAMv3.5a (Global Land Evaporation Amsterdam Model) dataset (Miralles et al., 2011) (https://www.gleam.eu/) were selected. Both CCI and GLEAM soil moisture are at 0.25° spatial resolution, and ERA5 soil moisture is at 0.1°.

The land cover dataset (Fig. 1b) was provided by the Data Center for Resources and Environmental Sciences, Chinese Academy of Sciences (RESDC) (https://www.resdc.cn) at about 1–km resolution (Liu et al., 2014). The dataset was produced using Landsat images, and contains 6 primary land use/land cover categories (Table 1). The proportions of each land cover type are listed in Table 1. One remarkable feature of this data is that paddy fields and dry fields are separated in the cropland group. The RESDC data is generated roughly every five years, and the 2015 data was selected for this study. The adjacent pixel method was used to convert the RESDC data to the sinusoidal projection of MODIS EVI.

Crop mapping with specifical crop type information is always a challenging academic task. We searched the sown area and yield of winter wheat at the county level in the statistical yearbook. Considering the uncertainty of statistics, we also used two data sets about planting area of winter wheat, both of which were extracted based on phenological methods. Dong et al. developed the planting area of winter wheat with a resolution of 30 m, and Luo et al. developed the planting area of wheat with a resolution of 1 km (Dong et al., 2020; Luo et al., 2020). The planting area of winter wheat of these two data sets were counted at the county level. It should be pointed out that the sown area represents the area of winter wheat that farmers had during the winter wheat sown season (last October), while the planting area refers to the area of winter wheat that year based on remote sensing monitoring.

2.3. Analysis processing

After a survey of historical records, the extreme precipitation event in October 2016 was chosen for analysis. This region has undergone a rapid process of agricultural modernization, with significant changes in the agricultural landscape over the decade. To highlight the impact of the current extreme event, we chose not to consider an overly long historical period. Instead, we opted for the years immediately before and after the occurrence of this extreme event as a reference. Therefore, the period from 2014 to 2018 was selected as the reference period for calculating monthly anomalies.

A threshold of 100 mm in precipitation monthly anomalies for October 2016 compared to the average of 2014–2018 was used to approximate the spatial extent of the event for convenience of analysis (illustrated by the red line in Fig. 1). Further analyses were conducted in this area defined by the 100 mm anomaly threshold. Although the threshold of 100 mm is somewhat subjective, it is roughly consistent with the 200 mm extension in October 2016. Importantly, precipitation in October 2016 was the historical maximum (264 mm in the regional average, greater than the mean plus four standard deviations) from 1961 to 2018 based on CMA data records. Meanwhile, the precipitation in October 2016 was higher than the multi-year average for July, the month with the highest average precipitation. Therefore, this is a very typical extreme case.

We first analyzed the general climate and vegetation characteristics of the area, and then selected the period of October 2016 to June 2017 to demonstrate the response of vegetation (mainly EVI) to the precipitation extremes. In addition, we also analyzed the sown area, planting area, yield of winter wheat and SIF to further confirm the correlation between the EVI anomalies in 2017 and precipitation extremes in 2016. The change in yield of winter wheat was expressed by the difference between the 2016 and 2017 growing seasons of EVI and SIF (the mean of March to May). At the same time, we used the sown area of winter wheat in 2016 minus sown area of winter wheat in 2015 to reflect the change in sown area of winter wheat caused by extreme precipitation in October 2016. Accordingly, we also use the planting area (yield) of winter wheat in 2017 minus planting area (yield) of winter wheat in 2016 to reflect the change in planting area (yield) of winter wheat caused by the change in sown area of winter wheat. If these changes are consistent, then we have established a direct link between extreme precipitation and changes in planting area (yield) of winter wheat, that is, between extreme precipitation and changes in EVI.

3. Results

3.1. Seasonal characteristics

During the period of 2014–2018, only one peak per year was found in the temperature, precipitation, and natural vegetation EVI records (Fig. 2a–c), with their maxima occurring in July (Table 2). Temperature in the coldest month (January) was still above zero, at 3.24 °C. Precipitation exhibited large interannual variations for each month, especially October due to the extreme case in 2016. The seasonal variations in natural vegetation maintained close consistency with these conditions.

However, a typical bimodal seasonal cycle was observed over the croplands, including both paddy field and dry croplands (Fig. 2d–f, Table 2). In croplands, the peaks in EVI occurred in April and August; the EVI in August represented the yearly maximum. The EVI of paddy fields were generally lower than those of dry croplands from January to May. This could reflect either the difference in plant types or the proportions of sowing. However, EVI for paddy fields and dry croplands both reached their lowest values in June during summer. Therefore, compared with natural vegetation, the bimodal distribution of EVI for cropland was presumed to be caused by agricultural rotations rather than the natural factors of precipitation and temperature.

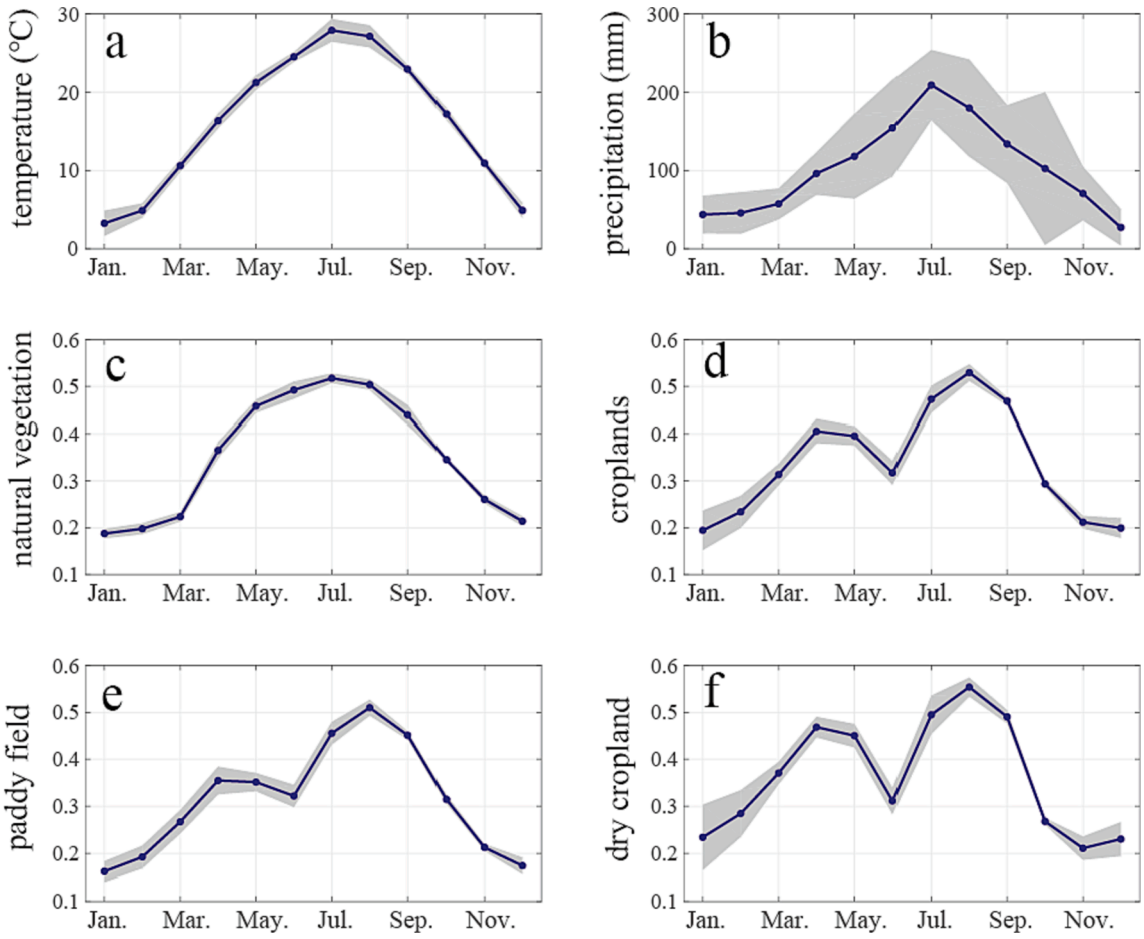

Fig. 2. Seasonal cycles of monthly temperature (a), precipitation (b), and EVI of natural vegetation (c), croplands (d), paddy field (e), and dry cropland (f) of the study region which is framed by the red line in Fig. 1 during 2014–2018. The blue curved lines indicate the monthly averages, with one standard deviations indicated by the shaded grey areas.

Table 2
Statistical characteristics of seasonal cycles of temperature, precipitation, and EVI.

Variable	Maxima (month)		Minima (month)	
Temperature	28.9 °C (Jul.)		3.24 °C (Jan.)	
Precipitation	209 mm (Jul.)		27 mm (Dec.)	
EVI–Natural	0.518 (Jul.)		0.187 (Jan.)	
EVI–Crop	0.406 (Apr.)	0.547 (Aug.)	0.317 (Jun.)	0.194 (Jan.)
EVI–paddy field	0.355 (Apr.)	0.527 (Aug.)	0.322 (Jun.)	0.162 (Jan.)
EVI–dry cropland	0.469 (Apr.)	0.554 (Aug.)	0.312 (Jun.)	0.211 (Nov.)

3.2. Response to the extreme precipitation

To characterize the response of vegetation to the precipitation extremes, the spatial and temporal patterns corresponding to a period of vegetation response to the precipitation extremes (i.e., October 2016 to June 2017) were illustrated on a monthly basis (Fig. 3). This period was selected because it covers the extreme precipitation events in October 2016 and extends until the summer harvest occurring in June.

Fig. 3 illustrates monthly anomalies in precipitation, temperature, and EVI for the period from October 2016 to June 2017. In October 2016, strong positive precipitation anomalies occurred in Eastern China, primarily within a triangular area (Fig. 3a1). Daily, 7–day, and 15–day regional average precipitation levels were calculated to demonstrate the temporal distribution (Fig. 4). Continuous precipitation began at the end of September. In October, 18 out of 31 days had an average daily rainfall exceeding 5 mm, leading to the continuity in October precipitation levels in the 7–day and 15–day smooth curves. This also indicates that soil moisture was continuously maintained at a high level, in contrast to a single flood event where the flood water quickly recedes after rainfall. Therefore, waterlogging disasters could be triggered by such rainfall distribution patterns, which would inevitably exert serious impacts on seeding. The temperature anomalies in this area were negative in the west and positive in the east (Fig. 3b1). However, EVI did not exhibit any clear and spatially consistent anomaly (Fig. 3c1). Due to the low EVI during the harvest season, it seems apparent that cropland vegetation did not respond much to this extreme event.

In the following winter months (from December 2016 to February 2017), precipitation did not show strong anomalies. Temperature was generally warmer than usual, especially in December 2016. During the same period, EVI exhibited a positive anomaly in the north, with the maximum occurring in February. There were no significant anomalies observed in the other regions.

The period from March to May is the essential period in which winter crops grow most vigorously (Fig. 2). However, in this case, from March to May 2017, EVI exhibited obvious negative anomalies over most of the region (Fig. 3c6–c8). Although there were some fluctuations in precipitation and temperature during March to May, precipitation is at 47 mm, 73 mm and 75 mm respectively, and temperature is at 9.6 ℃, 17.0℃ and 22.1℃ respectively. Therefore, no agricultural droughts and heatwaves were detected. The spatial pattern of the negative EVI anomalies was consistent with the spatial extent of the extreme precipitation in October 2016. However, in June 2017, EVI suddenly exhibited strong positive anomalies over the entire region (Fig. 3c9). Thus, it appears that the

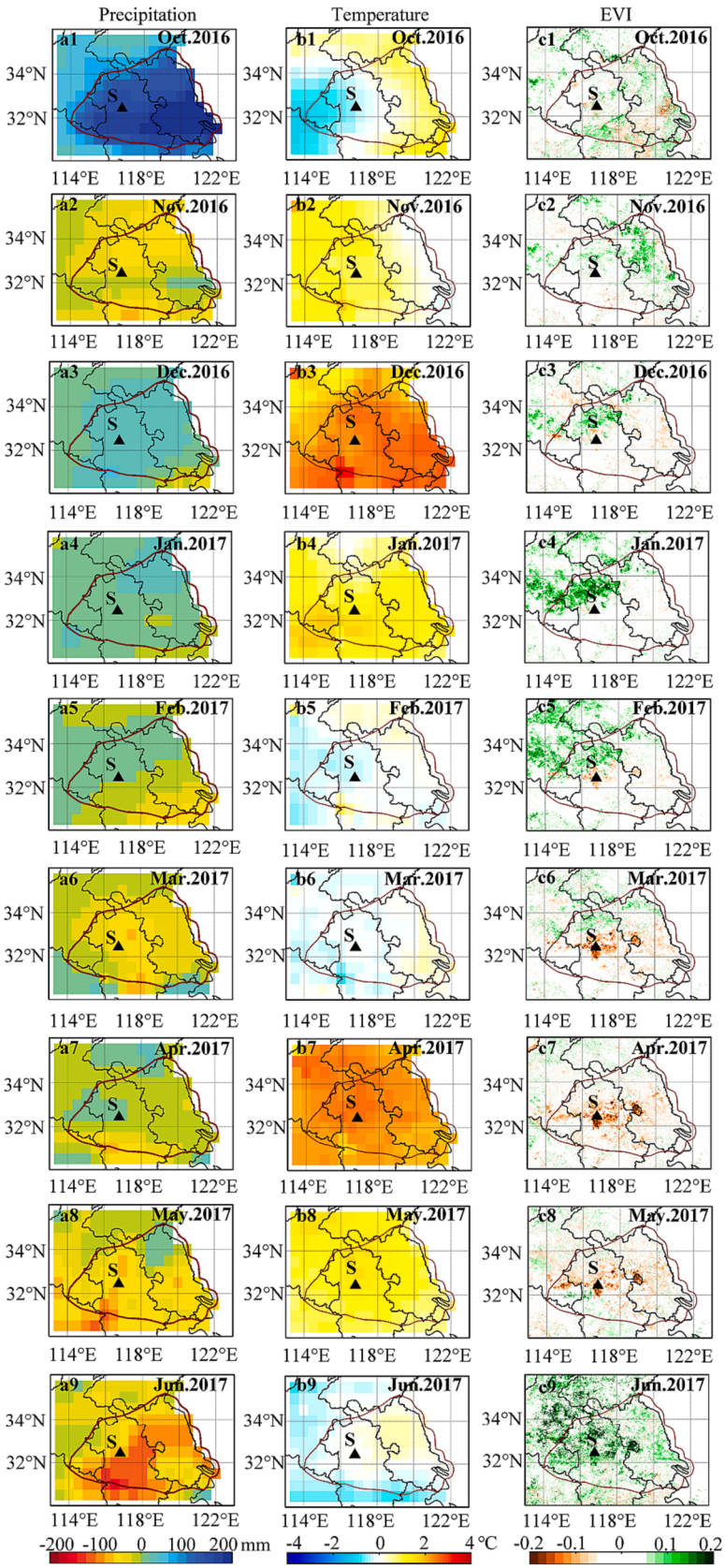

Fig. 3. Monthly anomalies in gridded precipitation (left column of panels, mm month^{-1}), temperature (middle column of panels, ℃), and EVI (right column of panels, unitless), from October 2016 to June 2017. A 100 mm precipitation anomaly was selected as the threshold to map the approximate spatial extent of extreme precipitation in October, which is indicated by the red boundary line.

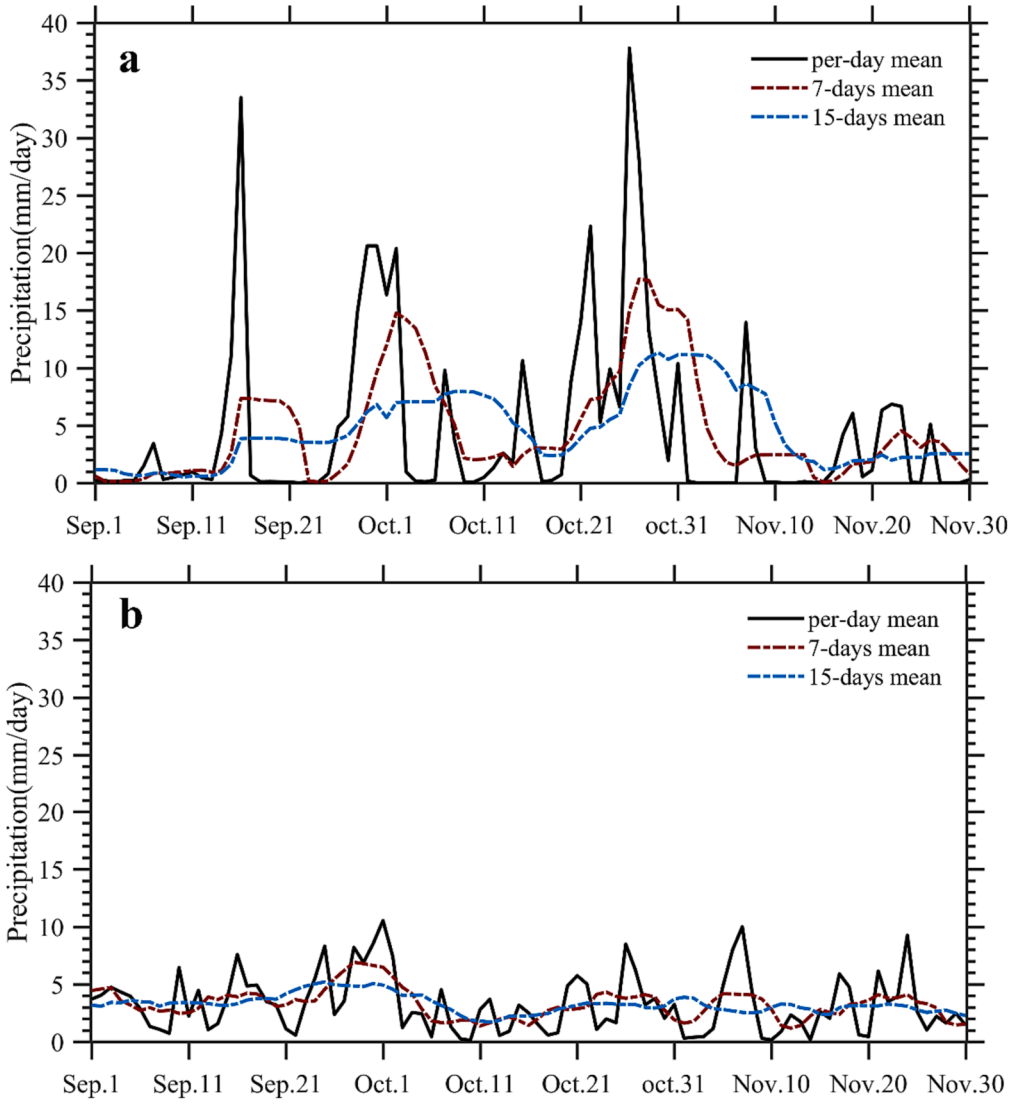

Fig. 4. Daily (black), 7–day (red), and 15–day (blue) mean precipitation from September to November 2016 (a) and the average values during 2014–2018 (b) of the region identified in Fig. 3 a1. (For interpretation of the references to colour in this figure legend, the reader is referred to the web version of this article.)

impact of the extreme precipitation on vegetation ended around that time.

The responses of vegetation to the extreme precipitation event were further analyzed according to different land cover types. Fig. 5 illustrates the regionally averaged anomalies in EVI, precipitation, and temperature. The EVI of cropland showed negative anomalies from March to May 2017. The behaviors of paddy fields and dry cropland were not consistent. Specifically, the negative anomalies in paddy fields were very obvious, and included November 2016 and February to May 2017. For the dry croplands, strong negative anomalies only appeared in April and May 2017, with the March anomaly being insignificant; the other months exhibited positive EVI values. The EVI values of paddy fields and dry croplands demonstrated consistent positive anomalies in June 2017. The magnitude of this anomaly was lesser than that of the croplands. At the same time, the only negative anomaly in the first half of 2017 occurred in April (Fig. 5). Therefore, the extreme precipitation event in October 2016 mainly negatively affected cropland vegetation rather than natural vegetation. The impact on paddy fields was thus obviously greater than it was on dry croplands.

3.3. Relationship between EVI anomalies and extreme precipitation

In order to confirm the correlation between EVI anomalies and extreme precipitation, winter wheat related data in the study area were further analyzed. County-level statistics showed a significant consistency between changes in sown area and yield of winter wheat, especially in areas where sown area of winter wheat declined, such as some parts of the central and southern regions (Fig. 6 a-b). This means that the change in yield of winter wheat is only related to the sown area of winter wheat. In other words, the decrease in yield of winter wheat in 2017 was due to a decrease in the sown area of winter wheat in October 2016. Fig. 7 shows the changes of planting areas of winter wheat generated based on remote sensing. Although not entirely consistent with county-level statistics, both data sets showed a widespread decline in planting area of winter wheat in some parts of the central and southern regions in 2017.

Compared with these winter wheat datasets, EVI declines were more widespread (Fig. 6c), which occurred in the central and southern regions. The decline was most pronounced in some parts of the central regions, where EVI declined by more than −0.1. The three SIF datasets showed results that are highly consistent with EVI, with declines in CSIF and RTSIF exceeding −0.3 and GOSIF around −0.1 in some parts of the

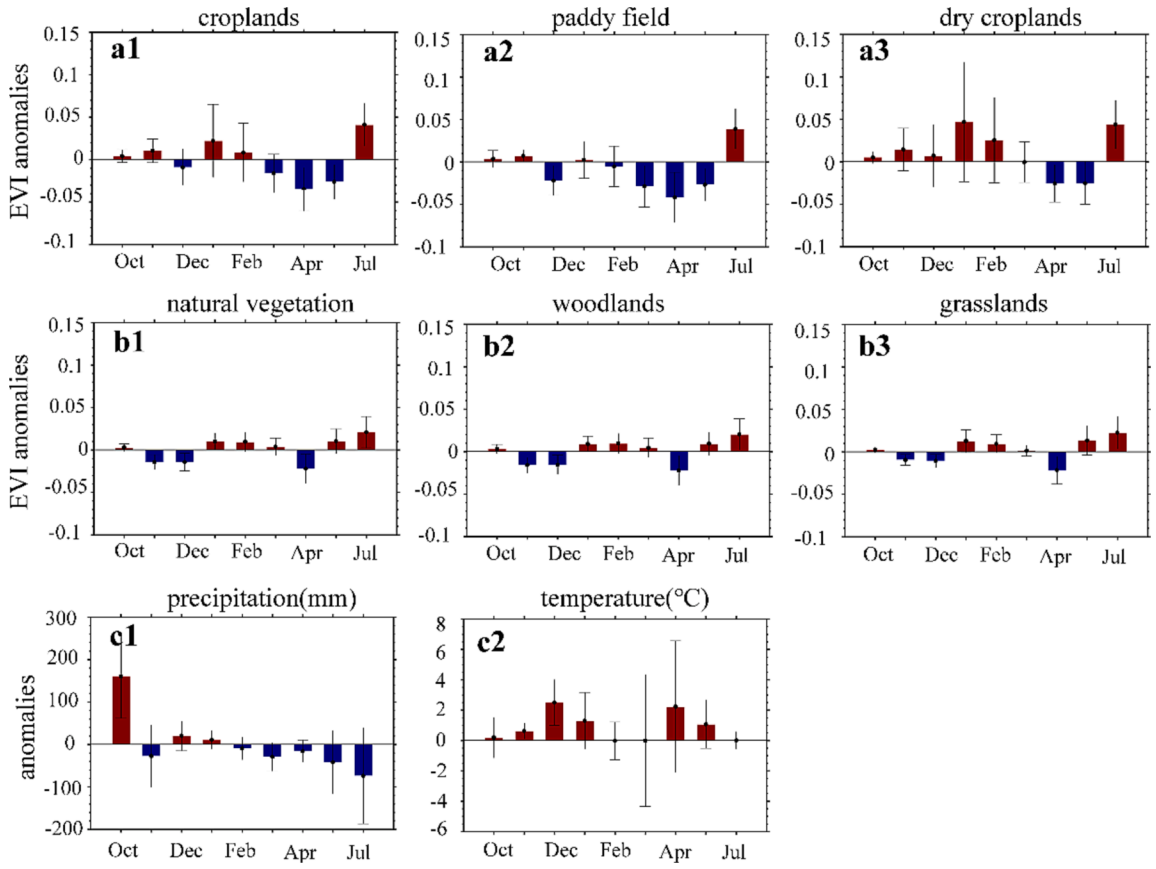

Fig. 5. Monthly anomalies in regionally averaged EVI, precipitation, and temperature from Oct.2016 to Jun. 2017: a1–a3 (upper row of panels) indicate EVI anomalies of all croplands, paddy fields, and dry croplands, respectively; b1–b3 (middle row of panels) indicate EVI anomalies in natural vegetation, woodlands, and grasslands, respectively; and c1–c2 (bottom row of panels) indicate the precipitation and temperature anomalies. Error bars indicate the standard deviations of each month during 2014–2018.

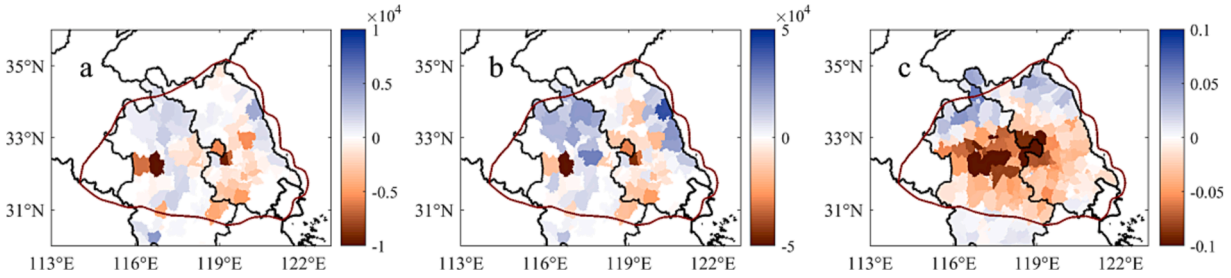

Fig. 6. Changes in sown area and yield of winter wheat and EVI at the county level. (a) and (b) are change in sown area (2016 minus 2015) and yield (2017 minus 2016) of winter wheat, respectively. (c) is change in mean EVI from March to May (2017 minus 2016). The sown area and yield of winter wheat in some regions is missing.

central regions (Fig S1). In some regions where yield increased, EVI and SIF showed inconsistent decrease, which may be due to some uncertainties in the statistical yield or climate-influenced fluctuations in EVI and SIF.

Despite some inconsistencies, all data sets show that crop growth (yield of winter wheat, EVI, SIF) was significantly lower in 2017 than in 2016 in some parts in the central and southern regions. By direct comparison with sown area and planting area of winter wheat, we suggest that one possible mechanism is that waterlogging disasters triggered by extreme precipitation had severely affected the sowing and seedling emergence (planting area) of winter crops (mainly winter wheat), thus affecting crop growth (EVI in this study) in 2017.

3.4. *Further evidence supporting the potential mechanism*

As a historical event, it is no longer possible to conduct field investigations. Therefore, we have further searched relevant documents and reports. We also surveyed the agricultural meteorological bulletins of some provinces and cities in the study area. The Anhui Meteorological Bureau announced in its monthly agricultural meteorological report that a continuous heavy rainfall in October 2016 had caused waterlogging disasters in the central and southern parts of the province, which severely affected the sowing of winter wheat and rapeseed. In northern Anhui, planting of winter wheat was almost completed as usual (Table S1). This further confirms the negative EVI anomalies which were mainly observed in the central and southern regions.

Information released by the Shouxian Meteorological Bureau (SMB)

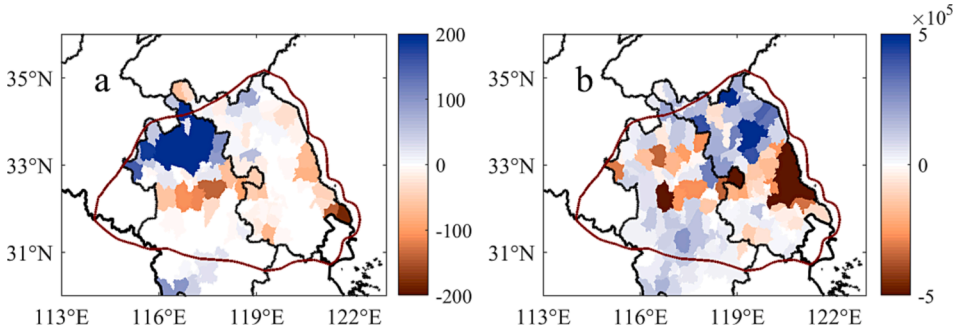

Fig. 7. Changes in planting area of winter wheat at the county level. (a) is change in planting area of winter wheat developed by Luo et al (2017 minus 2016), (b) is change in planting area of winter wheat developed by Dong et al (2017 minus 2016).

states that the yield reduction for winter wheat was mainly due to the lack of sowing caused by the extreme precipitation event, and the weather conditions during the growth period were generally good according to the SMB's report (Table S1). As illustrated in Fig. S2– Fig. S4, the photos of the surroundings were taken on March 29, 2017, with a roof of the observation station as the center–point. It can be seen clearly that both inside and outside the station, a large amount of cropland had been abandoned (lack of sowing), and were instead covered with very small grasses. We also tried to locate some sown winter wheat fields. The distribution of winter wheat on the ground appeared mottled (low seedling emergence rate), indicating that the germination of seedlings during the sowing period was seriously negatively affected (Fig. S2–Fig. S4). Rapeseed was in the flowering period (yellow flowers), and was mainly planted on the edges of the fields.

4. Discussion

Climate extremes seriously threaten global agricultural production and could affect significantly on terrestrial carbon cycle (Lesk et al., 2016; Piao et al., 2019; Reichstein et al., 2013). DC systems are expected to continue to expand in the future, and are regarded as one of the most effective ways to increase food production (Liu et al., 2013; Seifert and Lobell, 2015). This paper presents a potential benchmark case involving DC systems, suggesting a newly reported mechanism for the impact of extreme climate events on vegetation, namely that land management extends the duration of the impacts of extreme climate events on vegetation in double–cropping systems.

4.1. Robustness of the potential mechanism

To firmly establish the causality of waterlogging disasters caused by extreme precipitation during the sowing period and negative vegetation anomalies in spring, the suspicion of serious negative effects on EVI led by other climatic factors during the growing season of winter crops need to be ruled out. In this article, it specifically refers to whether the high temperature (about + 2 °C) and low precipitation that occurred in April and May 2017 as shown in Fig. 3 caused a heatwave or a drought. Indeed, precipitation is not very low during these two months at 73 mm and 75 mm respectively. Temperature is also far from "hot", at 17.0℃ and 22.2℃ of each. A paper which is an official agricultural meteorological briefing released by the National Meteorological Centre (Zhang et al., 2017), confirmed that April and May are relatively warmer and sunnier, which helps to significantly improve the negative effects of insufficient light caused by early continuous rainfall (Table S1). Therefore, the spring climatic conditions are very conducive to the growth of winter crops.

Soil moisture condition is essential in agriculture water availability, which usually has not efficient direct ground observations for regional scale application. Here, three soil moisture datasets were selected (see Methods). As illustrated in Fig. 8, all data showed that in the first 3–4 months, soil moisture had been maintained at a high level. Since the spring of 2017, soil moisture had shown a downward trend. During the period from March to May, the soil moisture in the southern part of the study area was significantly higher than that in the northern part, and the above–mentioned decline in EVI was mainly concentrated in the southern area. This further proves that the high temperature and low precipitation from March to May did not cause drought, nor was it the cause of the decline in EVI during the same period. One thing that needs to be explained is that the reasons for the abnormally high–value areas in the northern and southern parts of the study area shown by the ERA5 data are still unclear.

4.2. Comparison with other extreme events

In general, the damage to vegetation caused by extreme drought is significant. However, the response of vegetation to extreme precipitation may be different. In some systems with limited water resources, ecological processes are primarily driven by precipitation, and extreme precipitation events further promote vegetation growth (He et al., 2023). In some humid and subhumid areas, extreme precipitation does not promote or even inhibit the growth of vegetation. Previous studies have highlighted various mechanisms. For instance, extreme precipitation has been reported to disrupt soil stability, resulting in a decrease in vegetation biomass (Qu et al., 2023). Additionally, insufficient solar radiation and waterlogging, stemming from extreme precipitation, have significantly impeded vegetation photosynthesis (Chen et al., 2023). The adverse effects of extreme precipitation on crop yields are multifaceted, encompassing direct physical damage and processes linked to excessive soil moisture, such as waterlogging and flooding (Li et al., 2019). Notably, these mechanisms are primarily associated with climate change and seldom address land management. Our study delves further into the ways in which extreme precipitation impacts vegetation, shedding light on crucial insights. This holds particular significance for forecasting models related to crop yield, given that existing process-based models have been noted to inadequately capture yield losses resulting from extreme precipitation (Li et al., 2019).

In this study, the mechanism we proposed reflects more of a lagged effect of vegetation response to land management under extreme events, that is, the current land management affects the vegetation change in the subsequent period of time. A similar mechanism has been reported in previous studies in Europe's extreme drought of 2018, in which a warm spring climate promoted vegetation growth and intensified soil water consumption, which in turn amplified summer drought (Bastos et al., 2020). Again, this mechanism is very similar to the well-known legacy effects of drought, which are extremely prevalent in temperate and boreal forests worldwide (Anderegg et al., 2015). Therefore, whether this mechanism is widespread in DC croplands around the world needs to be further explored in the future.

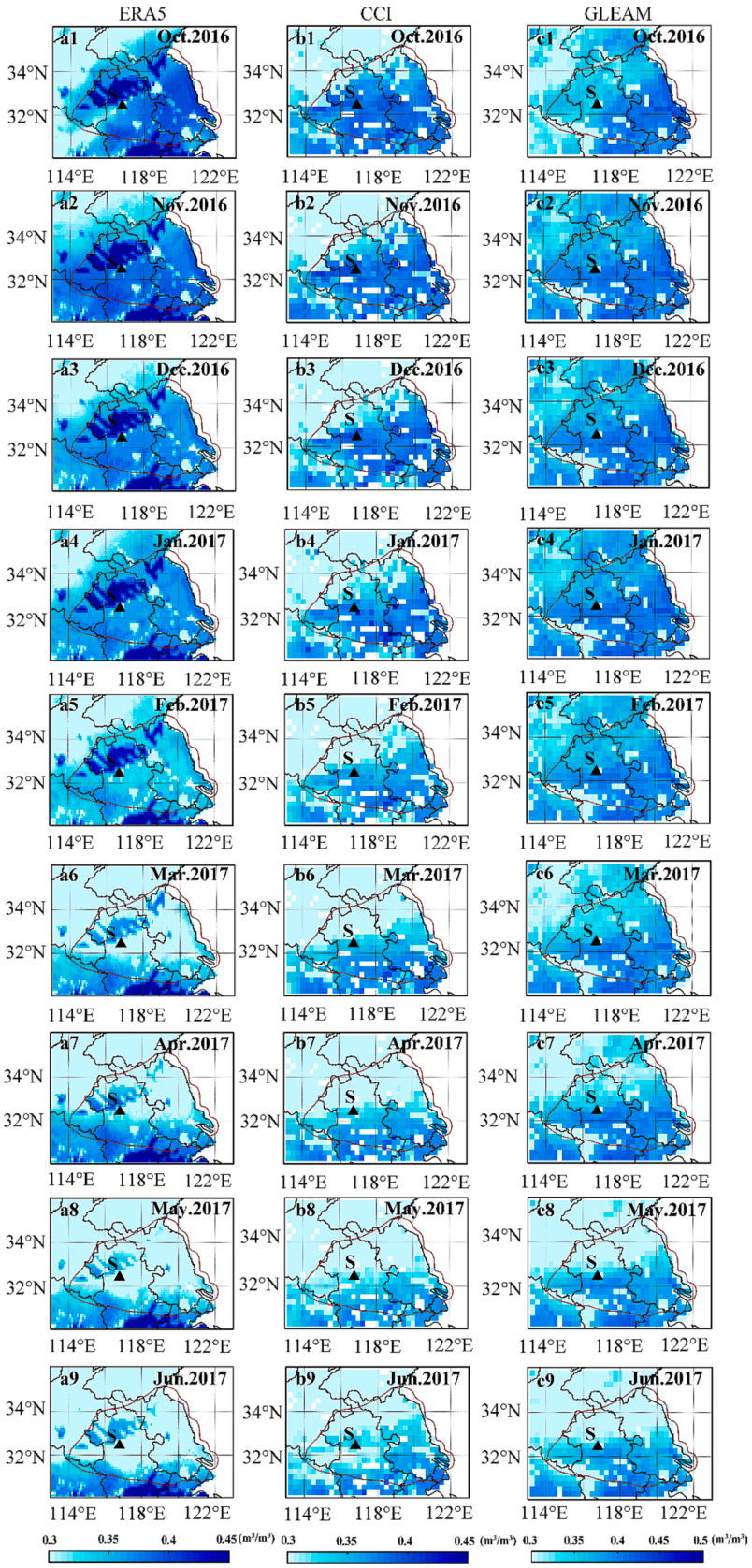

Fig. 8. Monthly soil moisture from ERA5 reanalysis (left column of panels), CCI and GLEAM with the unit of m^3/m^3 during October 2016 to June 2017.

4.3. Implication of the potential mechanism

From the information gathered above, it was confirmed that the EVI anomalies in some parts of the central and southern regions illustrated in Fig. 3, particularly those from March to May 2017, were mainly caused by the extreme precipitation event in October 2016. Thus, the impact on vegetation lasted 8 months, and the time period is clearly quantifiable in this case.

The waterlogging disaster induced by the extreme precipitation events which inhibited sowing was also influenced by the soil conditions. This is reflected in the differences in the responses to this extreme event between vegetation in dry croplands and that in paddy fields, as shown in Fig. 5. As illustrated by the photos in Fig. S2–Fig. S4, in the DC field of 'winter wheat–paddy rice', winter wheat was planted by broadcast seeding rather than by drill seeding in lines by machines. One basic reason for the necessity for broadcast seeding is that the soil of paddy fields has a very high water–holding capacity and is very sticky; it is not suitable for agriculture machinery sowing operations. Therefore, the impact of extreme precipitation during the sowing period of winter wheat in the paddy rice DC systems was more severe than that in the dry croplands DC systems.

Food demand is expected to increase continuously in the future. Increasing plant intensity, for example by using methods such as multiple cropping, is an important way to enhance food production, especially as it does not require increased cropland area. In the context of global warming, the areas suitable to DC systems have expanded and are expected to continue to expand. At the same time, in the future, the frequency and intensity of extreme precipitation will increase (Myhre et al., 2019; Tabari, 2020). Therefore, the risk of the mechanism illustrated herein, by which croplands may be negatively affected under similar future scenarios, needs to be assessed in subsequent studies.

4.4. Limitations and prospects

Although our study demonstrates the impact of land management on vegetation during extreme precipitation, we did not use some of the statistical or modeling methods used in previous studies (Chen et al., 2023; Li et al., 2019). On the one hand, most of the previous studies proved the impact of climate change on crops, but rarely involved land management, so it is easy to obtain a strong correlation between climate factors and crop yield. However, this may be applicable to our study, because the accurate quantification of the impact of land management on vegetation is still a research blank, which needs further exploration and exploration (Chen et al., 2019). On the other hand, because the impact of land management on vegetation is difficult to quantify accurately, the current models rarely contain the module of land management, especially for yield models, so it is difficult to use modeling methods to analyze.

5. Conclusion

In conclusion, we established a case study to systematically analyze the impact of extreme precipitation on cropland vegetation during the sowing period. The extreme precipitation that occurred in October 2016 led to a serious decline in winter wheat sowing. This resulted in a significant negative anomaly in the vegetation index of the winter wheat growth season in spring of the following year. These negative anomalies lasted until June 2017, when the next summer crops were planted. As indicated by the vegetation index, the impact of the precipitation extreme was most pronounced in April and May, lagging the precipitation extreme by more than 6 months. Our discoveries broaden the understanding of how extreme precipitation affects cropland vegetation, potentially advancing the development of vegetation models over agricultural areas. The impact area of this mechanism will expand in the future due to the increasing demand for grain production, the expansion of areas suitable for double-season planting, and the anticipated increase in extreme precipitation events. However, the threshold for triggering such a mechanism still needs further research in order to provide a reasonable reference value for future risk analysis.

Author contributions

T.C. and H.D. designed the study. T.C., J.D., H.M., C.L., S.Z., T.S., and X.C. collected the data and performed the analysis. C.D., Y.F., and T.N. recorded observations and assisted the field survey in the Shouxian National Climate Observatory. F.Z. and X.W. contributed to the extreme mechanism explanation. All authors contributed to the interpretation of the results and jointly revised the manuscript.

CRediT authorship contribution statement

Tiexi Chen: Conceptualization, Data curation, Formal analysis, Investigation, Methodology, Project administration, Supervision, Writing – original draft, Writing – review & editing. **Jie Dai:** Data curation, Formal analysis, Writing – original draft, Writing – review & editing. **Xin Chen:** Data curation, Formal analysis, Writing – original draft, Writing – review & editing. **Chuanzhuang Liang:** Data curation, Formal analysis, Methodology, Software, Visualization, Writing – original draft. **Tingting Shi:** Data curation, Validation, Writing – original draft. **Yanran Lyu:** Data curation, Writing – original draft. **Fang Zhao:** Data curation, Writing – original draft. **Xiuchen Wu:** Formal analysis, Methodology, Writing – original draft. **Miaoni Gao:** Formal analysis, Writing – original draft. **Jinlong Huang:** Data curation, Writing – original draft. **Shengjie Zhou:** Data curation, Writing – original draft. **Han Dolman:** Conceptualization, Methodology, Writing – original draft.

Declaration of competing interest

The authors declare that they have no known competing financial interests or personal relationships that could have appeared to influence the work reported in this paper.

Data availability

Data will be made available on request.

Acknowledgments

This research is supported by the Natural Science Foundation of Qinghai Province (NO. 2023-QLGKLYCZX-10), the National Natural Science Foundation of China (NO. 42130506, 42161144003, 31570464). A.J. Dolman acknowledges support from the program of the Netherlands Earth System Science Centre (NESSC), financially supported by the Ministry of Education, Culture and Science (OCW) (grant 024.002.001). The authors thank the China Meteorological Data Service Center (http://data.cma.cn) and the Resources and Environmental Science Data Center (RESDC) of the Institute of Geographic Sciences and Natural Resources Research, Chinese Academy of Sciences, for data provision. We thank the colleagues Yong HUANG, Chunfeng DUAN, Yan FENG and Ting NI in Anhui Provincial Meteorological Bureau for their help in data collection.

Appendix A. Supplementary data

Supplementary data to this article can be found online at https://doi.org/10.1016/j.ecolind.2023.111488.

References

AghaKouchak, A., Cheng, L., Mazdiyasni, O., et al., 2014. Global warming and changes in risk of concurrent climate extremes: Insights from the 2014 California drought. Geophys. Res. Lett 41, 8847–8852. https://doi.org/10.1002/2014GL062308.

Allen, C.D., Macalady, A.K., Chenchouni, H., et al., 2010. A global overview of drought and heat-induced tree mortality reveals emerging climate change risks for forests. For. Ecol. Manage 259, 660–684. https://doi.org/10.1016/j.foreco.2009.09.001.
Anderegg, W.R., Berry, J.A., Smith, D.D., et al., 2012. The roles of hydraulic and carbon stress in a widespread climate-induced forest die-off. P. Natl. Acad. Sci. USA 109, 233–237. https://doi.org/10.1073/pnas.1107891109.
Anderegg, W.R., Schwalm, C., Biondi, F., et al., 2015. Pervasive drought legacies in forest ecosystems and their implications for carbon cycle models. Science 349 (6247), 528–532.
Bastos, A., Ciais, P., Friedlingstein, P., et al., 2020. Direct and seasonal legacy effects of the 2018 heat wave and drought on European ecosystem productivity. Sci. Adv. 6 (24), eaba2724.
Bolton, D.K., Friedl, M.A., 2013. Forecasting crop yield using remotely sensed vegetation indices and crop phenology metrics. Agric. For. Meteorol. 173, 74–84.
Bowman, D.M., Williamson, G.J., Abatzoglou, J.T., et al., 2017. Human exposure and sensitivity to globally extreme wildfire events. Nat. Ecol. Evol 1, 1–6. https://doi.org/10.1038/s41559-016-0058.
Bussmann, A., Elagib, N.A., Fayyad, M., et al., 2016. Sowing date determinants for Sahelian rainfed agriculture in the context of agricultural policies and water management. Land Use Policy 52, 316–328.
Cao, J., Zhang, Z., Tao, F., et al., 2021. Integrating multi-source data for rice yield prediction across china using machine learning and deep learning approaches. Agric. For. Meteorol. 297, 108275.
Chen, T., de Jeu, R., Liu, Y., et al., 2014. Using satellite based soil moisture to quantify the water driven variability in NDVI: A case study over mainland Australia. Remote Sens. Environ 140 (140), 330–338. https://doi.org/10.1016/J.RSE.2013.08.022.
Chen, T., Wang, G., Yuan, W., et al., 2016. Asymmetric NDVI trends of the two cropping seasons in the Huai River basin. Remote Sens. Lett 7, 61–70. https://doi.org/10.1080/2150704X.2015.1109156.
Chen, T., Guo, R., Yan, Q., et al., 2022a. Land management contributes significantly to observed vegetation browning in Syria during 2001–2018. Biogeosciences 19, 1515–1525. https://doi.org/10.5194/bg-19-1515-2022.
Chen, T., Dolman, H., Sun, Z., et al., 2022b. Land management explains the contrasting greening pattern across china-russia border based on paired land use experiment approach. J. Geophys. Res. Biogeosci. 127 (6), e2021JG006659.
Chen, X., Huang, Y., Nie, C., et al., 2022c. A long-term reconstructed TROPOMI solar-induced fluorescence dataset using machine learning algorithms. Sci. Data 9 (1), 1–11.
Chen, C., Park, T., Wang, X., et al., 2019. China and India lead in greening of the world through land-use management. Nat. Sustainability 2 (2), 122–129.
Chen, J., Qiu, B., Guo, W., Li, L., Miao, X., 2023. Divergent response of crops and natural vegetation to the record-breaking extreme precipitation event in 2020 modulated by topography. Environ. Res. Lett.
Ciais, P., Sabine, C., Bala, G., et al., 2014. Carbon and other biogeochemical cycles. Climate change 2013: the physical science basis. In: Contribution of Working Group I to the Fifth Assessment Report of the Intergovernmental Panel on Climate Change. Cambridge University Press, pp. 465–570. https://doi.org/10.1017/-CBO9781107415324.004.
Dong, J., Fu, Y., Wang, J., et al., 2020. Early-season mapping of winter wheat in China based on Landsat and Sentinel images. Earth Syst. Sci. Data 12 (4), 3081–3095. https://doi.org/10.5194/ESSD-12-3081-2020.
Easterling, D.R., Meehl, G.A., Parmesan, C., et al., 2000. Climate extremes: observations, modeling, and impacts. Science 289, 2068–2074. https://doi.org/10.1126/science.289.5487.2068.
Erb, K.-H., Luyssaert, S., Meyfroidt, P., et al., 2016. Land management: data availability and process understanding for global change studies. Glob. Change Biol 23. https://doi.org/10.1111/gcb.13443.
Fischer, E.M., Beyerle, U., Knutti, R., 2013. Robust spatially aggregated projections of climate extremes. Nat. Clim. Change 3, 1033–1038. https://doi.org/10.1038/nclimate2051.
Friedlingstein, P., Jones, M.W., O'Sullivan, M., et al., 2019. Global carbon budget 2019. Earth Syst. Sci. Data 11, 1783–1838.
Gaba, S., Lescourret, F., Boudsocq, S., et al., 2015. Multiple cropping systems as drivers for providing multiple ecosystem services: from concepts to design. Agron. Sustain. Dev 35. https://doi.org/10.1007/s13593-014-0272-z.
Guan, K., Berry, J.A., Zhang, Y., et al., 2016. Improving the monitoring of crop productivity using spaceborne solar-induced fluorescence. Glob. Change Biol. 22 (2), 716–726.
He, L., Guo, J., Yang, W., Jiang, Q., Chen, L., Tang, K., 2023. Multifaceted responses of vegetation to average and extreme climate change over global drylands. Sci. Total Environ. 858, 159942.
Hersbach, H., de Rosnay, P., Bell, B., et al., 2018. Operational global reanalysis: progress, future directions and synergies with NWP. Retrieved from. https://www.ecmwf.int/node/18765.
Ho, C.H., Park, S.J., Jeong, S.J., et al., 2012. Observational evidences of double cropping impacts on the climate in the Northern China plains. J. Clim. 25, 4721–4728. https://doi.org/10.1175/JCLI-D-11-00224.1.
Huete, A., Didan, K., Miura, T., et al., 2002. Overview of the radiometric and biophysical performance of the MODIS vegetation indices. Remote Sens. Environ. 83, 195–213. https://doi.org/10.1016/S0034-4257(02)00096-2.
Jabal, Z.K., Khayyun, T.S., Alwan, I.A., 2022. Impact of climate change on crops productivity using MODIS-NDVI time series. Civil Eng. J. 8 (06).
Karthikeyan, L., Chawla, I., Mishra, A.K., 2020. A review of remote sensing applications in agriculture for food security: crop growth and yield, irrigation, and crop losses. J. Hydrol. 586, 124905.
Katz, R.W., 2010. Statistics of extremes in climate change. Clim. Change 100, 71–76. https://doi.org/10.1007/s10584-010-9834-5.
Lesk, C., Rowhani, P., Ramankutty, N., 2016. Influence of extreme weather disasters on global crop production. Nature 529, 84–87. https://doi.org/10.1038/nature16467.
Li, Y., Guan, K., Schnitkey, G.D., DeLucia, E., Peng, B., 2019. Excessive rainfall leads to maize yield loss of a comparable magnitude to extreme drought in the United States. Glob. Change Biol. 25 (7), 2325–2337.
Li, X., Xiao, J., 2019. A global, 0.05-degree product of solar-induced chlorophyll fluorescence derived from OCO-2, MODIS, and reanalysis data. Remote Sens. (Basel) 11 (5), 517.
Liu, Y.Y., Dorigo, W.A., Parinussa, R.M., et al., 2012. Trend-preserving blending of passive and active microwave soil moisture retrievals. Remote Sens. Environ 123, 280–297. https://doi.org/10.1016/J.RSE.2012.03.014.
Liu, J.Y., Kuang, W.H., Zhang, Z.X., et al., 2014. Spatiotemporal characteristics, patterns, and causes of land-use changes in China since the late 1980s. J. Geog. Sci 24, 195–210. https://doi.org/10.1007/s11442-014-1082-6.
Liu, L., Xu, X., Zhuang, D., Chen, X., et al., 2013. Changes in the potential multiple cropping system in response to climate change in China from 1960–2010. PLoS One 8, e80990.
Loboda, T., Krankina, O., Savin, I., Kurbanov, E., Hall, J., 2017. Land management and the impact of the 2010 extreme drought event on the agricultural and ecological systems of European Russia. Land-Cover and Land-Use Changes in Eastern Europe after the Collapse of the Soviet Union in 1991, 173–192.
Luo, Y., Zhang, Z., Li, Z., et al., 2020. Identifying the spatiotemporal changes of annual harvesting areas for three staple crops in China by integrating multi-data sources. Environ. Res. Lett. 15 (7), 074003.
Luyssaert, S., Jammet, M., Stoy, P., et al., 2014. Land management and land-cover change have impacts of similar magnitude on surface temperature. Nat. Clim. Chang 4, 389–393. https://doi.org/10.1038/nclimate2196.
Marteau, R., Sultan, B., Moron, V., et al., 2011. The onset of the rainy season and farmers' sowing strategy for pearl millet cultivation in Southwest Niger. Agric. for. Meteorol 151, 1356–1369. https://doi.org/10.1016/j.agrformet.2011.05.018.
Miralles, D.G., Holmes, T.R.H., Jeu, R.A.M., et al., 2011. Global land-surface evaporation estimated from satellite-based observations. Hydrol. Earth Syst. Sci 15 (2), 453–469. https://doi.org/10.5194/HESS-15-453-2011.
Myhre, G., Alterskjær, K., Stjern, C.W., et al., 2019. Frequency of extreme precipitation increases extensively with event rareness under global warming. Sci. Rep. 9 (1), 16063.
Pan, Y., Birdsey, R.A., Fang, J., et al., 2011. A large and persistent carbon sink in the world's forests. Science 333, 988–993. https://doi.org/10.1126/science.1201609.
Peng, B., Guan, K., Zhou, W., et al., 2020. Assessing the benefit of satellite-based solar-induced chlorophyll fluorescence in crop yield prediction. Int. J. Appl. Earth Obs. Geoinf. 90, 102126.
Piao, S., Zhang, X., Chen, A., et al., 2019. The impacts of climate extremes on the terrestrial carbon cycle: a review. Sci. China Earth Sci. 62, 1551–1563. https://doi.org/10.1007/s11430-018-9363-5.
Qu, Q., Xu, H., Ai, Z., et al., 2023. Impacts of extreme weather events on terrestrial carbon and nitrogen cycling: a global meta-analysis. Environ. Pollut. 319, 120996.
Reichstein, M., Bahn, M., Ciais, P., et al., 2013. Climate extremes and the carbon cycle. Nature 500, 287–295. https://doi.org/10.1038/nature12350.
Seifert, C.A., Lobell, D.B., 2015. Response of double cropping suitability to climate change in the United States. Environ. Res. Lett 10, 024002. https://doi.org/10.1088/1748-9326/10/2/024002.
Siebert, S., Portmann, F.T., Döll, P., 2010. Global patterns of cropland use intensity. Remote Sens 2, 1625–1643. https://doi.org/10.3390/rs2071625.
Sillmann, J., Kharin, V.V., Zwiers, F., et al., 2013. Climate extremes indices in the CMIP5 multimodel ensemble: Part 2. Future climate projections. J. Geophys. Res. Atmos 118, 2473–2493. https://doi.org/10.1002/jgrd.50188.
Skakun, S., Franch, B., Vermote, E., et al., 2017. Early season large-area winter crop mapping using MODIS NDVI data, growing degree days information and a Gaussian mixture model. Remote Sens. Environ. 195, 244–258.
Smith, M., 2011. An ecological perspective on extreme climatic events: a synthetic definition and framework to guide future research. J. Ecol 99, 656–663. https://doi.org/10.1111/j.1365-2745.2011.01798.x.
Tabari, H., 2020. Climate change impact on flood and extreme precipitation increases with water availability. Sci. Rep. 10 (1), 13768.
Tilman, D., Balzer, C., Hill, J., et al., 2011. Global food demand and the sustainable intensification of agriculture. PNAS 108, 20260–20264. https://doi.org/10.1073/pnas.1116437108.
Ummenhofer, C.C., Meehl, G.A., 2017. Extreme weather and climate events with ecological relevance: a review. Philos. Trans. R. Soc. London, Ser. B 372, 20160135. https://doi.org/10.1098/rstb.2016.0135.
USGS., 1996. Global 30 Arc-Second Elevation (GTOPO30), Available online at: https://www.usgs.gov/centers/eros/science; doi: /10.5066/F7DF6PQS.
Vermeulen, S.J., Campbell, B.M., Ingram, J.S., 2012. Climate change and food systems. Annu. Rev. Environ. Resour 37. https://doi.org/10.1146/annurev-environ-020411-130608.
Wu, X., Liu, H., Li, X., et al., 2018. Differentiating drought legacy effects on vegetation growth over the temperate Northern Hemisphere. Global Change Biol 24, 504–516. https://doi.org/10.1111/gcb.13920.
Xu, Y., Gao, X., Shen, Y., et al., 2009. A daily temperature dataset over China and its application in validating a RCM simulation. Adv. Atmos. Sci 26, 763–772. https://doi.org/10.1007/s00376-009-9029-z.
Yan, H., Xiao, X., Huang, H., et al., 2014. Multiple cropping intensity in China derived from agro-meteorological observations and MODIS data. Chin. Geogr. Sci. 24, 205–219. https://doi.org/10.1007/s11769-013-0637-2.

Yin, Y., Byrne, B., Liu, J., Wennberg, P. O., Davis, K. J., Magney, T., Köhler, P., He, L., Jeyaram, R. & Humphrey, V. 2020. Cropland carbon uptake delayed and reduced by 2019 Midwest floods. AGU Advances, 1, e2019AV000140. doi: 10.1029/2019AV000140.

Zhai, P., Sun, A., Ren, F., et al., 1999. Changes of climate extremes in China. Clim. Change 42 (1), 203–218. https://doi.org/10.1023/A:1005428602279.

Zhang, L., Cheng, L., Zheng, C.L., et al, 2017. Impact of climate on agricultural production in spring 2017 (in Chinese). Chinese Journal of Agrometeorology. (07), 466-468, doi:CNKI:SUN:ZGNY.0.2017-07-008.

Zhang, Y., Joiner, J., Alemohammad, S.H., et al., 2018. A global spatially contiguous solar-induced fluorescence (CSIF) dataset using neural networks. Biogeosciences 15 (19), 5779–5800.

Zhou, S., Chen, T., Zeng, N., et al., 2022. The impact of cropland abandonment of post-soviet countries on the terrestrial carbon cycle based on optimizing the cropland distribution map. Biology 11 (5), 620.